International Journal of Innovative Computing, Information and Control
Volume **21**, Number **2**, April **2025**

ICIC International ©2025 ISSN 1349-4198
pp. **491–513**

UNMANNED AERIAL VEHICLE TO GROUND RISK ASSESSMENT BASED ON TARGET DETECTION

Sen Luo[1], Xingyu Cao[1], Qinggang Wu[2,3] and Pengxin Ding[1,*]

[1]School of Computer Science
Chengdu University of Information Technology
No. 24 Block 1, Xuefu Road, Chengdu 610225, P. R. China
{ 3220608041; 3220609001 }@stu.cuit.edu.cn; *Corresponding author: dpx@cuit.edu.cn

[2]The Second Research Institute of Civil Aviation Administration of China
[3]Civil Unmanned Aircraft Traffic Management Key Laboratory of Sichuan Province
No. 919, Linqi Avenue, Sancha Street, Eastern New Area, Chengdu 610041, P. R. China
wuqinggang@caacsri.com

Received December 2023; revised June 2024

Abstract. *Unmanned Aerial Vehicles (UAVs), as autonomous aerial systems, are increasingly being utilized in various applications. However, potential crash events of UAVs pose significant risks and safety concerns for public safety on the ground. This paper presents a comprehensive method for assessing ground risks during UAV operation by integrating the dynamic characteristics of the crash process and target detection techniques. First, the Monte Carlo method is employed to analyze the distribution of impact points during the UAV's ballistic descent and to calculate the probability distribution of various affected area sizes, estimating the likelihood of a UAV crash in different regions. Next, target detection is used to identify objects within the crash zone. Based on key factors related to public and property safety, detected objects are classified into three categories: people, vehicles, and other objects. The hazard levels of these categories are combined with the model results to compute the ground risk value during UAV operation. Finally, simulation results validate the approach by demonstrating that combining the spatial distribution of the crash zone with target detection of different object types can effectively assess the ground risk during UAV operation. Unlike methods that rarely consider the actual risks to the ground post-crash, our approach integrates risk identification, quantification, and evaluation. By combining probabilistic risk assessment, the Monte Carlo method, and deep learning technologies, a more comprehensive and accurate risk assessment is achieved.*

Keywords: Unmanned Aerial Vehicle (UAV), Risk assessment, Small object detection, Monte Carlo method

1. **Introduction.** In recent years, with the rapid growth of the UAV industry, the scope of UAV applications has continually expanded, leading to increased societal concern over UAV safety risks [1, 2]. In this context, managing UAV operations has become critically important, and operational risk assessment is a key component. Unlike manned aircraft, the most distinguishing characteristic of UAVs is that they are unmanned. As a result, in UAV risk assessments, the focus shifts away from the safety of onboard personnel, as in traditional aircraft, and towards the risks associated with UAV crashes caused by internal and external factors during flight, which pose potential threats to the lives and property of people on the ground [3]. In other words, UAV crashes, which threaten objects at ground impact sites, have become one of the primary risks for UAV operations in low-altitude

DOI: 10.24507/ijicic.21.02.491

airspace in China. This highlights the need for further research into UAV-related ground risks.

The core of UAV ground risk assessment lies in identifying and quantifying the factors that may lead to UAV crashes and evaluating their potential impact on ground targets. These factors include, but are not limited to, mechanical failures, operational errors, environmental conditions, and external interference. Some researchers have analyzed UAV failure causes from three perspectives: system failures, operating environments, and human factors. They use Bayesian networks to analyze the primary failure causes and their probabilities, facilitating ground risk assessments [4, 5, 6]. Given the complexity and interrelated nature of failure causes, this method effectively decomposes complex joint probability distributions into simpler submodules, reducing the complexity of probabilistic reasoning. However, Bayesian networks depend on accurate prior knowledge and data, and in practical applications-especially in emerging fields like UAVs-obtaining comprehensive and precise data can be challenging.

Therefore, one of the key challenges and research hotspots in UAV risk assessment is evaluating the ground risks and hazards posed to ground targets under failure conditions, based on the identification and quantification of UAV failure causes [7]. To address the safety risks posed by UAV operations, relevant institutions in various countries have developed standards and guidelines to regulate and improve UAV safety. For example, JARUS (Joint Authorities for Rulemaking on Unmanned Systems) has issued process guidance for Special Operations Risk Assessment (SORA) for specific UAV types [8]. The Civil Aviation Administration of China (CAAC) has published standards such as the "Trial Operation Management Regulations for Specific Types of Unmanned Aircraft (Interim)" [9] and the "Guidance on Unmanned Aircraft Airworthiness Certification Based on Operational Risk" [10] to regulate higher-risk UAV operations. Additionally, some studies classify UAV safety threats into internal and external categories, and propose risk mitigation methods accordingly [11]. These standards and guidelines have promoted the standardized development of the UAV industry and enhanced overall UAV safety. Moreover, scholars have explored the relationship between UAVs and ground targets, examining the ground risks posed to buildings, transportation routes, and pedestrians, as well as the varying levels of risk under different conditions [12]. These studies provide important references for developing comprehensive and effective risk management strategies.

To assess the ground safety of UAVs and estimate the risks associated with UAV crashes, several methods and algorithms have been proposed. Probabilistic risk assessment methods [7, 13] analyze the probability and consequences of each failure mode by examining UAV system failure modes and their impacts, thereby quantifying overall risk. Monte Carlo simulations, through extensive random sampling and simulation experiments, evaluate the risk levels under different scenarios [14, 15, 16]. Machine learning [17, 18] and deep learning [19, 20] techniques have also been applied in UAV ground risk assessment. By analyzing UAV flight and historical accident data, these techniques predict the likelihood of UAV crashes in different failure scenarios and assess their impact on ground targets. The application of machine learning and deep learning technologies allows UAV risk assessments to leverage large datasets of flight and environmental data, thereby constructing more accurate and dynamic risk models.

Despite the progress these methods have made in UAV ground risk assessment, there are still technical challenges and research gaps. First, data acquisition and data quality are key issues. In emerging application fields or under-researched scenarios, the lack of comprehensive and accurate data can affect the precision of risk assessments. Additionally, current assessment methods may be inadequate for handling highly dynamic and uncertain environments, making it difficult to capture UAV behavior and decision-making processes

fully. Addressing these challenges is essential for improving the reliability and accuracy of UAV risk assessments.

Our main contributions are summarized as follows.

- We developed a novel risk modeling method that combines the dynamic characteristics of the UAV crash process with target detection technology. This approach accounts for uncertainty factors in the crash process and uses target detection to identify objects within the crash zone, providing a more accurate assessment of crash impacts. This integrated method enables a more comprehensive and precise risk assessment, enhancing UAV operational safety.
- We constructed a comprehensive framework that integrates risk identification, quantification, and assessment, utilizing techniques such as probabilistic risk assessment, Monte Carlo simulations, and deep learning. Through detailed analysis of UAV system failure modes and flight environment data, we created a dynamic risk assessment model that can be continuously updated and optimized. This framework is designed to operate in highly dynamic and uncertain environments, improving both the accuracy and practical application of risk assessments.

The remainder of the paper is organized as follows. Section 2 reviews the current state of research on UAV ground risk assessment methods and their challenges. Section 3 outlines the methods employed in this study, including the use of Monte Carlo simulations to estimate UAV crash locations, deep learning for small object detection to identify risks, and grid-based representation of the crash zone. Section 4 presents experimental results and case analyses of the proposed ground risk assessment approach. Finally, Section 5 concludes the main findings of the study.

2. **Related Works.**

Risk assessment mainly relies on scientific methods and modeling to estimate the potential consequences of accidents, providing an accurate understanding of event safety. For UAVs, risk assessment is essential for determining whether they can safely integrate into the National Airspace System (NAS). With the development of Unmanned aircraft system Traffic Management (UTM) concepts, improving real-time safety assessment capabilities has gained increasing importance. To support the gradual integration of UAV systems into NAS, many researchers have conducted in-depth studies on UAV low-altitude operation risks. In the following, we review the current research status of UAV ground risk assessments and the challenges involved, categorizing them into qualitative and quantitative methods, and compare them with the approach proposed in this study.

2.1. **Qualitative methods.**

Qualitative risk assessment methods primarily rely on expert knowledge and experience, using non-quantitative analysis to identify and evaluate risks. These methods are typically applied in the early stages of risk assessment to providing an overall understanding and identification of potential risks. For instance, in some standards issued by JARUS and CAAC [8, 9, 10], risk matrices are used to represent the levels of risk by classifying and ranking the likelihood and severity of risks, allowing for effective risk evaluation and prioritization. Sivakumar et al. [21] developed a ground risk framework based on SORA, performing risk assessments by constructing risk matrices according to event probability and severity. Zhong et al. [22] proposed a model for ground fatalities and UAV crash-induced economic losses, constructing a risk assessment matrix, which was further used to generate risk maps. Risk maps, a commonly used qualitative tool, represent risk factors along UAV flight routes visually, providing an intuitive overview of overall risk. For example, Primatesta et al. [23, 24] considered factors such as

population density, shelter factors, and uncertainties, using risk maps to show the risks faced by the ground population when UAVs fly over specific areas (e.g., cities).

Qualitative methods are widely applied in UAV risk assessments due to their simplicity, cost-effectiveness, and minimal data requirements. Particularly in the early stages of risk identification and preliminary assessment, they provide quick and comprehensive risk overviews. However, as these methods rely on subjective judgment and expert experience, the results may suffer from some degree of subjectivity and uncertainty, making it difficult to provide precise quantitative risk data.

2.2. **Quantitative methods.** Quantitative risk assessment methods analyze data and models. The simplest approach involves calculating the probability of an accident, assessing its severity, and then multiplying these factors to obtain the risk value. Typically, ground fatalities are used as the risk evaluation standard, with additional considerations for impact area, shielding factors, population density, and fall probability. For example, Avanzini and Martínez [25] assessed the ground impact risk following a UAV system failure, using system reliability (failure rate per unit time), population density, and the position of the impact point. A fatal area is defined under certain conditions, and risk is quantified based on the time each point on the ground spends within the fatal area. This approach innovatively combines risk quantification with the time factor. Qi [26] developed a UAV ground impact risk model based on two dimensions of risk factors: the probability and severity of the risk. This model considers the UAV operation risk coefficient and uses fatalities from ground impact as an indicator. It also accounts for different UAV operational scenarios, providing references for various operational conditions. Han and Zhao [27] introduced environmental impact factors and developed a UAV ground impact accident model, using the number of fatalities per flight hour as a metric. Zhang et al. [28] constructed a UAV collision safety risk model based on equivalent safety levels, with ground population density as the core, offering a feasible approach for UAV system risk evaluation. McFadyen et al. [29] used the Australian Advanced Air Traffic System (TAAATS) radar to collect aircraft position reports and quantified UAV collision risks by analyzing overlap probabilities of manned and unmanned aircraft in each space unit. By combining real monitoring data with advanced statistical methods, this approach enables more accurate UAV collision risk quantification. Zhou et al. [30] proposed a quantitative ground risk assessment mechanism, extracting urban ground features from high-resolution satellite images to create multi-layered risk maps considering factors like population density, shielding, and ground obstacles. They calculated pedestrian, vehicle, and property risks for each unit and generated 3D risk maps with a resolution of 1m $\times$ 1m $\times$ 5m. The study also introduced resolution conversion methods to adapt to various UAV operation needs. Case studies showed that the fifth and tenth layers had lower risks, making them more suitable for UAV operations.

Quantitative methods rely on data and models, providing more precise risk assessment results. They play an important role in detailed evaluations and decision support. However, these methods often require large amounts of data and complex calculations, and face challenges in data acquisition and quality.

Overall, current research on UAV ground risks primarily focuses on evaluating the risks during UAV operations, based on the probability of UAV failure and the severity of the resulting consequences. However, few studies consider the actual ground risks after UAV failures, particularly in cases of UAV collisions with the ground. Therefore, this study aims to use the Monte Carlo method to estimate the UAV crash impact area, and apply object detection technology to identifying objects that may be affected within this area, providing a realistic assessment of UAV ground risks.

To verify the main safety analysis methods applied in the field of UAV risk assessment in recent years, these methods have been summarized in Table 1. Each method has distinct advantages and disadvantages in addressing UAV risk assessment.

Table 1. Comparison of risk assessment methods

Risk assessment method	Advantages	Disadvantages
This study method	Considers the UAV crash dynamics and target detection technology, enabling more precise assessment of potential impacts of crash accidents, and dynamically updates based on UAV system failure modes and flight environment data.	The process involves risk identification, quantification, and assessment, which necessitate substantial computational resources.
Probability risk assessment	Quantifies overall risk by analyzing UAV system failure modes and impacts.	Does not consider the dynamic nature of UAV crash scenarios, relatively simple calculations.
Monte Carlo simulation	Handles uncertainties in UAV crashes through extensive random sampling and simulation experiments to assess risks.	Requires both significant computational resources and a complex simulation process.
Machine learning	Analyzes and models UAV flight data and historical accident data to predict crash probabilities and their impacts on ground targets.	Difficulties in data acquisition and processing, complex model training.
Bayesian networks	Analyzes major failure factors and their occurrence probabilities, and decomposes complex joint probability distributions.	Relies on accurate prior knowledge and data support, challenging to obtain comprehensive and precise data in practical applications.

The method proposed in this paper integrates the dynamic characteristics of a UAV's descent with actual ground conditions, providing a comprehensive reflection of the potential impact of crash incidents. The assessment results are dynamically updated based on changes in the flight environment. Although this approach requires relatively high computational resources, it offers higher applicability and accuracy in real flight conditions, demonstrating significant advantages.

3. **Methods.** Through a review of relevant domestic and international literature, it is found that research on UAV ground risk assessment can be broadly categorized into the following stages: UAV failure model, impact area prediction model, ground population distribution model, and hazard assessment model. The UAV failure model aims to analyze various failure modes that may occur during UAV flight and calculate the UAV's flight trajectory under different failure conditions. The impact area prediction model forecasts the possible crash area after UAV failure. By considering flight dynamics and environmental conditions, the trajectory of the UAV in the event of failure is simulated to determine potential impact points. The ground population distribution model constructs a detailed map of population distribution based on demographic data, dynamically reflecting changes in population density over time and location, which is critical for assessing

the risk UAV crashes pose to ground populations. The hazard assessment model evaluates the potential consequences of UAV impacts on ground targets. In this study, we replace the traditional ground population distribution model with object detection technology to identify and assess objects within the crash area. Unlike static population models, this new method can dynamically acquire real-time information on the crash area, including not only population density but also other potential affected ground targets, thereby significantly enhancing the comprehensiveness and accuracy of ground risk assessment.

3.1. **UAV failure model.** After encountering airborne failure, a UAV may exhibit several different crash modes. La Cour-Harbo [13, 31] analyzed and summarized these modes, including ballistic descent, parachute descent, uncontrolled glide, and flyaway. In the ballistic descent mode, the UAV loses most of its lift and enters a ballistic-like descent state, which is the most common crash mode after UAV failure. The parachute descent mode occurs when, following a system failure, the engine shuts down, and an onboard parachute is deployed, relying on parachute aerodynamics to reduce descent speed and mitigate the threat to ground objects. The uncontrolled glide mode describes the situation where a fixed-wing UAV loses power but retains structural integrity, gliding freely toward the ground. In this mode, the UAV utilizes its remaining aerodynamic properties to glide to the ground. The flyaway mode refers to the situation where the operator completely loses control of the UAV, and the autopilot continues to operate in a flight-stability-maintaining mode. The UAV's flight path is then controlled by the autopilot and can fly in any direction until its maximum flight range is reached. This mode is characterized by an uncertain flight path, which may pose a broader potential threat to ground targets [32].

3.2. **UAV crash location estimation.** Currently, there are two main methods for predicting the crash point of a UAV after failure: the empirical estimation method and the modeling analysis method. The empirical estimation method relies on UAV characteristics, such as mass, size, and historical failure data, often referencing similar cases of UAV failures to estimate the flight path and the potentially affected area. In contrast, the modeling analysis method primarily uses aerodynamic and kinematic models to predict the crash trajectory and applies probability distribution functions to calculating the potential extent of the affected area after UAV failure.

Since ballistic descent is the most common crash mode after UAVs encounter airborne failures, and this mode is easier to model and analyze, it allows for the comprehensive consideration of UAV-related parameters and environmental forces (such as wind speed) that influence the descent trajectory. Therefore, this study proposes to adopt the UAV ballistic descent mode in conjunction with the modeling analysis method to determine the approximate range of the UAV's ground impact point. This approach will accurately study the descent process of UAVs after airborne failure and provide scientific evidence to support UAV flight safety.

The crash forms associated with internal UAV system failures typically include free-fall or projectile motion in a loss of control or power state. In consideration of the air resistance during descent, the UAV's landing process is modeled. The motion of the UAV after the crash is decomposed into horizontal and vertical components, and the following motion equations are derived [33]:

$$\begin{cases} m\dfrac{d^2x}{dt^2} = -F_x \\ m\dfrac{d^2y}{dt^2} = G_{uav} - F_y \end{cases} \tag{1}$$

In the equation, m represents the mass of the UAV; G_{uav} represents the gravity acting on the UAV; x represents the horizontal displacement of the UAV during falling; y represents the vertical displacement of the UAV during falling; t represents the falling time of the UAV; F_x represents the air resistance acting on the UAV in the horizontal direction; F_y represents the air resistance acting on the UAV in the vertical direction.

Detailed analysis of the aerodynamic drag experienced by the UAV reveals that the drag forces in the horizontal and vertical directions are as follows:

$$\begin{cases} F_x = \dfrac{1}{2} c S_x \rho \left(\dfrac{dx}{dt} \right)^2 \\ F_y = \dfrac{1}{2} c S_y \rho \left(\dfrac{dy}{dt} \right)^2 \end{cases} \tag{2}$$

In the equation, c represents the air resistance coefficient, ρ represents air density, S_x represents the windward area in the lateral direction of the UAV, and S_y represents the windward area in the vertical direction of the UAV.

Substituting Equation (2) into Equation (1) yields

$$\begin{cases} m \dfrac{d^2x}{dt^2} = -\dfrac{1}{2} c S_x \rho \left(\dfrac{dx}{dt} \right)^2 \\ m \dfrac{d^2y}{dt^2} = mg - \dfrac{1}{2} c S_y \rho \left(\dfrac{dy}{dt} \right)^2 \end{cases} \tag{3}$$

In the equation, g represents the gravitational acceleration.

Based on the initial conditions when the UAV crashes due to failure, i.e., $\begin{cases} v_{x_0} = v_0 \\ v_{y_0} = 0 \end{cases}$ and $\begin{cases} x_0 = 0 \\ y_0 = 0 \end{cases}$, where v_0 represents the initial velocity at the failure point when the UAV crashes, v_{x_0} represents the initial lateral velocity at the failure point when the UAV crashes, v_{y_0} represents the initial vertical velocity at the failure point when the UAV crashes, x_0 represents the initial lateral position at the failure point when the UAV crashes and y_0 represents the initial vertical position at the failure point when the UAV crashes. By integrating Equation (3) and substituting the initial conditions, the horizontal displacement of the UAV crash point from the failure point when the UAV crashes is obtained:

$$x = \frac{2m}{cS_x\rho} \ln \left(cS_x \rho v_0 t + 2m \right) - \frac{2m \ln(2m)}{cS_x \rho} \tag{4}$$

When the operating altitude of the UAV is known as h, its time of impact with the ground is given by the following equation:

$$t_{y=h} = \sqrt{\frac{2m}{cS_y \rho g}} \ln \left(\exp \left(\frac{cS_y \rho h}{2m} \right) \pm \sqrt{\exp \left(\frac{cS_y \rho h}{m} \right) - 1} \right) \tag{5}$$

The instantaneous velocity of the UAV at the moment of impact with the ground is

$$\begin{cases} v_x = \dfrac{2mv_0}{cS_x \rho v_0 t + 2m} \\ v_y = \sqrt{\dfrac{2mg}{cS_y \rho}} \tanh \left(\sqrt{\dfrac{cS_y \rho g}{2m}} t \right) \end{cases} \tag{6}$$

In the equation, v_x represents the horizontal velocity of the UAV at the moment of impact, and v_y represents the vertical velocity of the UAV at the moment of impact.

The kinetic energy of the UAV upon impact with the ground can be determined from the UAV's instantaneous velocity at the time of impact.

$$E_{uav} = \frac{1}{2}m\left(v_x^2 + v_y^2\right) \tag{7}$$

The actual impact point of the UAV's crash is randomly distributed around the predicted impact point, and its probability density function is governed by the statistical distribution of impact errors. As a result, the Monte Carlo method can be used to determine the collision impact area on the ground. When the UAV is flying with an initial horizontal velocity v_0 and height h, a 2D diagram of the fall trajectory is shown in Figure 1, illustrating the object's descent to the ground impact point.

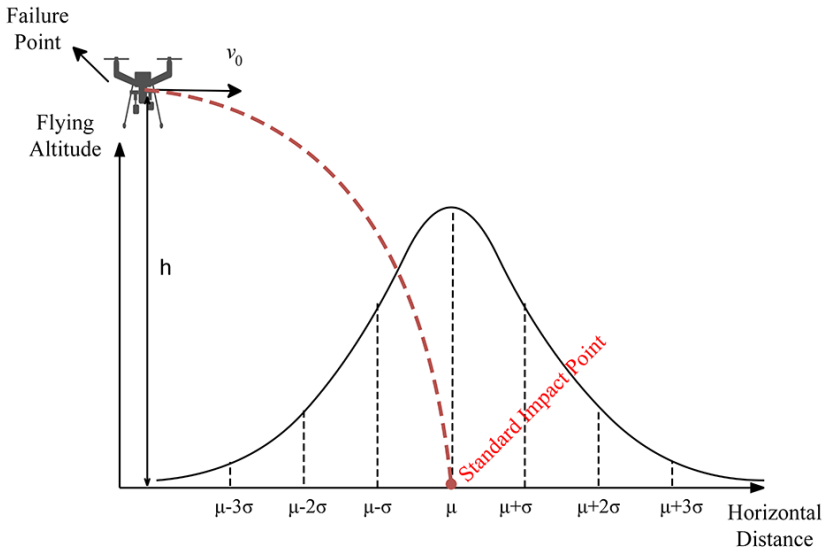

FIGURE 1. 2D schematic diagram of UAV crash impact points on the ground

3.3. **UAV ground object detection.**

3.3.1. *Data preparation.* UAVs equipped with cameras are extensively utilized in fields such as high-speed inspections, aerial photography, and surveillance. Consequently, the processing of visual data collected by UAVs demands high standards, leading to increasingly close integration between computer vision and UAV technology. Although UAVs offer a unique high-altitude perspective for detection tasks, images captured from such perspectives often encounter challenges, including significant changes in object scale and occlusions between objects. These challenges can lead to issues like false positives and missed detections when traditional object detection algorithms are applied. To address these challenges, researchers have proposed various optimizations to YOLOv5, resulting in a UAV-specific object detection method known as YOLO-UAV. This method enhances detection accuracy and efficiency by simplifying the network architecture, optimizing feature extraction, incorporating efficient feature fusion blocks, and introducing novel loss functions [34]. This optimization not only improves the accuracy and robustness of UAV-based object detection but also provides more reliable technical support for UAV applications in complex environments.

In response to the aforementioned challenges, this study utilizes the VisDrone-DET dataset [35]. Focused on small object detection in UAV aerial photography scenarios, the VisDrone-DET dataset was created and is maintained by the Chinese University of Hong Kong. The dataset was first released in 2018 and is continuously updated. It contains

images captured in various cities across China, featuring a diverse range of environments, objects (such as pedestrians and vehicles), and densities (ranging from sparse to crowded scenes). The dataset provides a rich variety of scenes and object categories, including 8,629 images captured by UAVs at various locations and altitudes. It is divided into training, validation, and test subsets: 6,471 images for training, 548 for validation, and 1,610 for testing. These images were collected from different locations but within similar environments, and the primary object categories for detection include pedestrian (1), people (2), bicycle (3), car (4), van (5), truck (6), tricycle (7), awning-tricycle (8), bus (9), and motor (10).

This study utilizes the VisDrone-DET dataset for the following reasons.

1) Data Collected from the UAV Perspective: The VisDrone-DET dataset is captured from a UAV's perspective, offering a wider and more comprehensive field of view compared to other datasets. This better aligns with the objectives of this research.

2) Large Scale and Diversity: The VisDrone-DET dataset contains a substantial amount of data collected by UAVs, covering a wide range of scenes, including variations from day to night and from urban to rural environments. This diversity makes it ideal for the object detection tasks required in this study.

3) Rich Annotations: The dataset provides detailed annotation information, including the location, size, and shape of objects. Additionally, it includes valuable metadata such as scene and time, which are directly aligned with the requirements of this research.

The distribution of the average width and height of the raw images in the training set, as well as the proportion of the average width and height of the bounding boxes relative to the actual image dimensions, is shown in Figure 2.

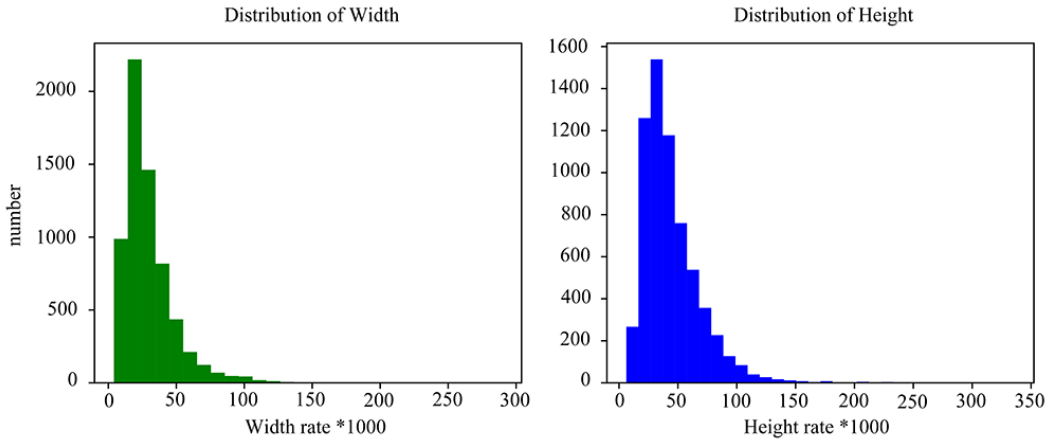

FIGURE 2. Average width-to-height ratio distribution of training set images

Based on the statistical analysis of the VisDrone-DET dataset, the average width and height of the original images with annotations are 1519.8895 pixels and 1002.397 pixels, respectively. The median ratios of the bounding box width to the original image width and the bounding box height to the original image height are 0.02465 and 0.03841, respectively. Thus, a cropping method is employed for training. The side length of the cropped sub-images is set to 640 pixels, ensuring a square shape after cropping, and the overlap rate between sub-images during cropping is set to 0.25, as shown in Figure 3.

3.3.2. *Model selection.* The field of small object detection currently faces several key challenges: the limited coverage area of small objects, the scarcity of effective features, the loss of information during downsampling, and difficulties in achieving model convergence.

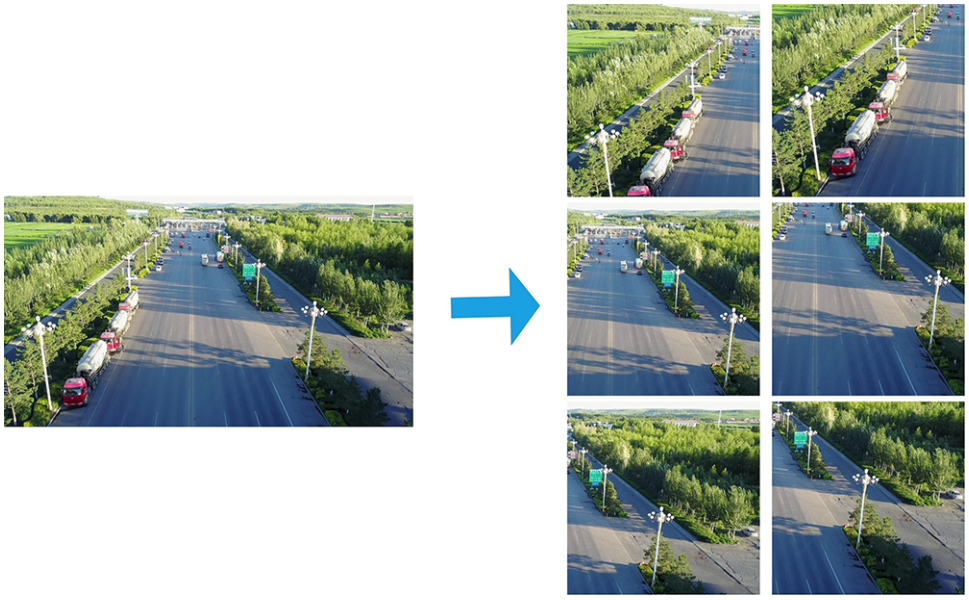

FIGURE 3. Image cropping of the training set

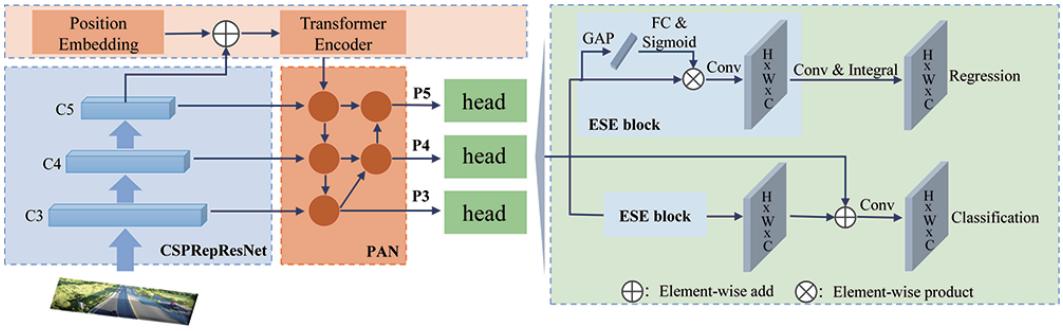

FIGURE 4. PP-YOLOE-SOD model diagram

Additionally, distinguishing similar targets in dense small-object regions remains a significant challenge. To address these issues, the Baidu PaddlePaddle Detection team has enhanced the general-purpose detection model PP-YOLOE and developed a specialized model for small object detection, PP-YOLOE-SOD (Small Object Detection) [36, 37, 38]. Compared to the PP-YOLOE model, the main improvement in PP-YOLOE-SOD is the introduction of a Transformer-based global attention mechanism in the neck part of the network. The use of Transformer models has gained significant attention in the field of computer vision. The Vision Transformer (ViT) model, for example, divides the image into multiple patches, incorporates positional embedding, and feeds these into a Transformer Encoder. When combined with appropriate classification or detection heads, this approach delivers excellent performance. In the PP-YOLOE-SOD model, the PaddleDetection team has also introduced two new modules: Position Embedding and Encoder. The architecture of the PP-YOLOE-SOD model is shown in Figure 4.

The PP-YOLOE-SOD model uses the same loss function design as the PP-YOLOE model, employing Varifocal Loss (VFL) as the classification loss function. This choice enables the model to focus more on high-quality samples during training, thereby improving classification performance. The model also uses Generalized Intersection over Union (GIoU) loss to evaluate the quality of the detection boxes, ensuring a high overlap between the predicted and ground truth boxes. To address the flexibility of bounding box

representation, the model introduces Distribution Focal Loss (DFL), which enhances the accuracy of object location prediction. These three loss functions are combined to form the overall loss function, as shown in Equation (8).

$$loss = \frac{\alpha \cdot loss_{VFL} + \beta \cdot loss_{GIoU} + \gamma \cdot loss_{DFL}}{\sum_{i}^{N_{pos}} \hat{t}} \tag{8}$$

In the equation, α, β, and γ are the weight parameters for $loss_{VFL}$, $loss_{GIoU}$, and $loss_{DFL}$, respectively, and $\hat{t}$ is the normalized target score.

In this framework, Varifocal Loss emphasizes the importance of positive samples, while GIoU loss improves spatial accuracy by considering the overlap between the predicted and ground truth boxes. DFL introduces the concept of distribution to enhance the flexibility of bounding box predictions, allowing the model to better accommodate objects of various shapes and sizes. The weighted combination of these loss functions makes the model more robust and efficient in tackling complex object detection tasks.

3.4. **Grid-based impact area and risk representation.** To effectively identify and address risks leading to harm or loss, this study combines object detection results with the probability of UAV crash impact points for risk assessment. The risk of different target categories is combined with the crash probability at specific locations. For each grid unit in the impact area, the corresponding risk value is calculated, and risk analysis is performed based on these values. The potential risk level of each grid unit is determined based on the risk values associated with the detected object types, thereby supporting risk assessment and decision-making. To achieve this, the method for assessing initial ground risk levels, as specified in the Civil Aviation Administration of China's "Regulations on the Trial Operation Management of Specific Types of UAVs (Interim)", divides ground risk into 11 levels. Based on this method and considering the context of this study, it is noted that in accident severity investigations, the impact of a UAV crash on personnel is far more significant than on property. Therefore, a risk value table is established, as shown in Table 2, which includes different target categories and their corresponding risk values. To identify and address the key risks that may cause harm or loss, special attention is given to two main target categories: people and vehicles. These categories typically represent the most significant risks from a UAV crash during flight. For other unclassified targets detected during the object detection process, they are categorized as "Others" and assigned relatively low risk values.

Table 2. Table of risk values

Category	Value
Person	10
Vehicle	6
Other	1

One of the main challenges in this study is dividing the impact area into manageable grid units for risk assessment. Grid-based partitioning is used to divide the impact area into regular grid cells, considering both the detected object categories within each grid and the probability of the UAV falling into that grid. These two factors are combined to calculate the potential risk level for each grid. The risk values are calculated based on the detection results of ground objects and the corresponding probability distribution factors determined earlier. Based on the accident severity standards, the following table is established.

TABLE 3. Accident severity classification standards

Value criteria	Severity of accidents
$[0, 1)$	Slight harm
$[1, 3)$	Moderate harm
$[3, 5)$	Severe harm

To facilitate grid division and risk assessment, an enclosing rectangle is introduced for the impact area based on prior calculations. The aim of this step is to simplify the shape of the impact area, making it easier to divide it into regular grid cells for risk assessment. By defining the enclosing rectangle, the impact area is divided into grid cells of equal size, with each cell representing a distinct region, thereby aiding subsequent risk assessment and data analysis. This approach ensures that the entire impact area is accounted for in the UAV crash risk assessment. The introduction of the enclosing rectangle improves the efficiency of risk analysis and calculations, ultimately enhancing decision support.

The UAV-captured image is processed into a grid, and the risk of the impact area is represented using a grid according to the hazard severity standards. Different colors are used to represent varying levels of hazard: green for minor hazards, orange for moderate hazards, and red for severe hazards. An example is shown in Figure 5.

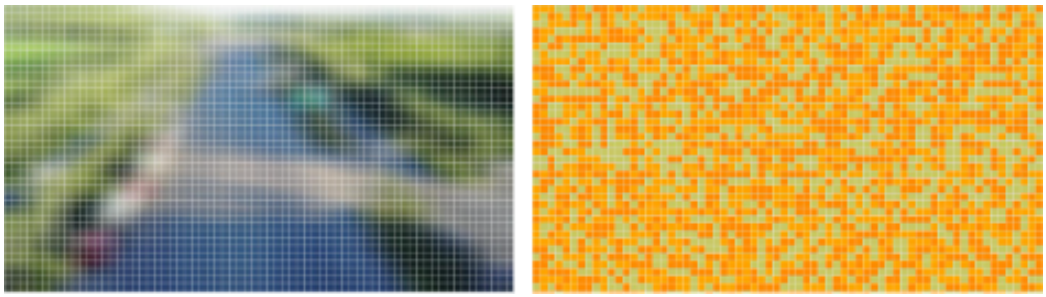

FIGURE 5. (color online) Grid representation of the crash landing area

The grid-based risk representation method provides a detailed and spatially precise risk assessment. Each grid cell represents a localized area within the ground impact zone, and this high-resolution evaluation is crucial when determining the UAV's landing site, as it accounts for varying impacts on people, vehicles, or other objects. The probability analysis of the impact area considers the likelihood of a UAV crash in each grid cell, taking account of uncertainty and dynamic factors to provide a comprehensive risk assessment. By integrating the probability of impact for each grid cell with the object detection results, a more thorough risk evaluation is achieved.

4. **Experiments and Case Study.** The ground risk associated with UAV failure scenarios is assessed. In the first part, the Monte Carlo simulation method is employed to analyze the distribution of UAV crash impact points under failure conditions. Environmental forces are shown to significantly influence crash locations, although impact points generally concentrate near the standard crash location. Using the 3σ criterion under the initial parameter settings, the probability distribution of various impact area sizes is calculated, representing the likelihood of a UAV falling into specific regions. In the second part, the PP-YOLOE-SOD model is trained and evaluated. The train subset of the VisDrone-DET dataset is segmented and used as training data, while the val subset serves as validation data. Analysis of the model's training loss shows steady improvement in target recognition and classification accuracy, demonstrating the model's strong

adaptability and robustness across different conditions. Finally, in combination with the previously described risk representation method, a UAV simulation model is developed to simulate crash patterns and ground risk assessment effects under specific conditions. This simulation analysis further validates the effectiveness of the proposed methods for UAV crash location distribution and risk assessment in failure scenarios.

4.1. **Crash location analysis.** In this section, the crash impact point distribution of UAVs under failure scenarios is simulated based on statistical data of UAV activities in China. Using specific initial conditions and the Monte Carlo simulation method, we analyze the characteristics of crash impact point distributions during UAV failures and their corresponding risk assessments. Experimental results indicate that environmental forces significantly influence UAV crash locations; however, the impact points are generally concentrated near the standard crash location. We also analyze the sizes of impact areas derived from different probability density functions and measure crash probabilities in various regions using the 3σ criterion.

According to statistical data [39], UAV activities in China are predominantly concentrated in low-altitude airspace, with the vast majority occurring at altitudes below 1000 m. Notably, UAV activities below 120 m account for 96.5% of the total. To better approximate real-world UAV failure scenarios, this study selects a flight altitude of 30 m and an initial horizontal velocity of 20 m/s as the basic simulation parameters. Rather than focusing on a specific commercial UAV model, this experiment uses the DJI Matrice M210-RTK UAV as a baseline reference, forming the foundation for this study. The initial conditions are ultimately set as shown in Table 4.

Table 4. Experimental initial conditions data

Parameters	Values
Mass	6.14 kg
Dimensions (length)	0.887 m
Dimensions (width)	0.880 m
Dimensions (height)	0.408 m
Lateral windward area	0.234 m^2
Vertical windward area	0.035 m^2
Altitude	30 m
Velocity	20 m/s
Aerodynamic drag coefficient	0.3
Air density	1.225
Gravity acceleration	9.8 m/s^2

Assuming the UAV's initial failure position is set as the origin of the coordinate system, a Cartesian right-hand coordinate system is defined, with the UAV's initial horizontal velocity along the positive x-axis and the z-axis pointing vertically downward. Simulating 100,000 initial positions for the UAV and combining Equation (4) with the influence of environmental forces during descent, the Monte Carlo simulation was employed to determine the distribution of UAV crash impact points, as shown in Figure 6. The impact points exhibit an elliptical pattern of distribution, indicating that the UAV's crash locations are randomly distributed within a certain range. This pattern reflects the influence of environmental forces, such as wind, during descent, causing the final impact points to deviate from the standard crash location.

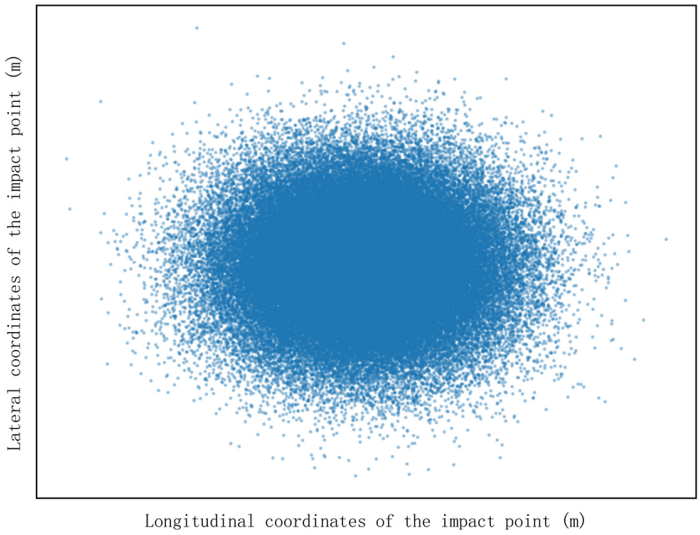

FIGURE 6. Monte Carlo simulation of UAV crash impact distribution

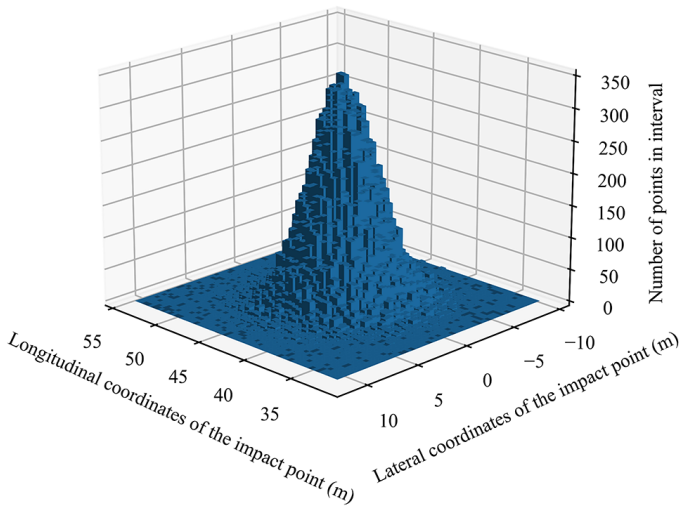

FIGURE 7. Distribution of UAV crash impact points

Based on the statistical data in Figure 7, the distribution pattern is concentrated and symmetrical around its center. The impact points are most concentrated near a longitudinal coordinate of 45 meters, while the lateral coordinate distribution symmetrically expands around 0 meters. This indicates that although environmental forces significantly influence the UAV's crash locations, the impact points predominantly remain within the vicinity of the standard crash location.

Taking the longitudinal distribution of crash impact points as an example, statistical data indicates that it conforms to a normal distribution with a mean of 42.7 m and a standard deviation of 2.48 m. The longitudinal distribution characteristics of crash impact points are illustrated in Figure 8.

The distribution of crash impact points and the affected area sizes vary depending on the probability density functions. To account for differences in UAV crash probabilities across different ground regions, the 3σ criterion for the impact area is employed to evaluate risk values for various airspace locations. The distribution of crash locations is categorized into three groups: S_σ, $S_{2\sigma}$, and $S_{3\sigma}$, ensuring comprehensive consideration of different risk

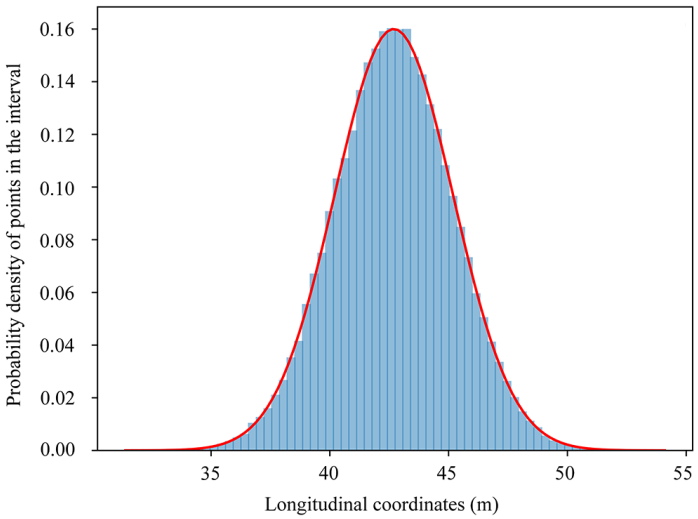

FIGURE 8. Longitudinal distribution of UAV crash impact points

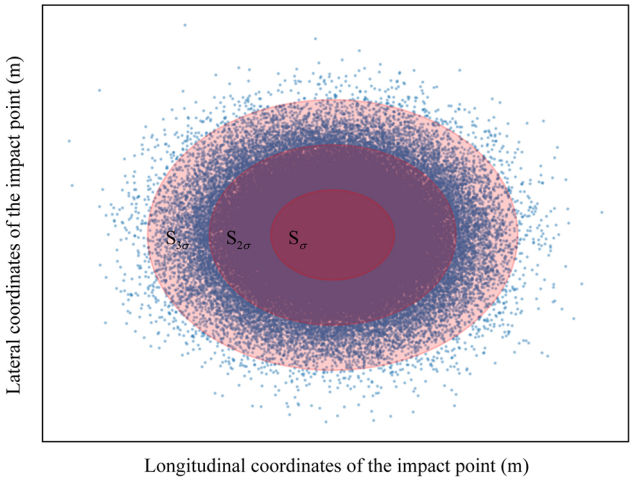

FIGURE 9. Impact area under different probability density functions

levels. Additionally, the impact area is discretized into n basic computational units, with corresponding risk values assigned to each unit based on small object detection data, forming a detailed risk representation. This method is expected to significantly enhance UAV safety and risk management by improving the accuracy of risk assessments, thereby increasing the safety and feasibility of UAV operations. Using the 3σ criterion, the mean values of the longitudinal and lateral distributions of crash impact points serve as the center, and the standard deviations in the longitudinal and lateral directions (multiplied by 1, 2, and 3) define the lengths of the major and minor axes. This approach delineates varying affected areas for the distribution of crash impact points, as shown in Figure 9.

Based on the calculations, the probability of crash impact points falling within the S_σ region is 46.64%, within the $S_{2\sigma}$ region is 91.11%, and within the $S_{3\sigma}$ region is 99.46%. Since UAV crashes in the three elliptical regions are mutually exclusive events, the probability of crash impact points falling between the S_σ and $S_{2\sigma}$ regions is 44.47%, while the probability of falling between the $S_{2\sigma}$ and $S_{3\sigma}$ regions is 8.35%. Thus, the probability of crash impact points falling outside S_σ, $S_{2\sigma}$, and $S_{3\sigma}$ region is 0.54%, which is considered negligible in this study.

To further quantify the risk values of different grid cells, using the described risk representation method, suppose the detected target category in a specific grid cell is "human", and the probability of a UAV crash in that cell is 46.64%. The corresponding risk value would be 4.6, indicating the risk for the "human" target at that location. Similarly, the risk values for other grid cells can be calculated using the same approach.

By integrating target detection results with UAV crash probabilities, this approach enables precise risk assessment for each grid cell. It not only facilitates the identification of high-risk areas but also provides essential insights for UAV flight decision-making.

4.2. **UAV ground object detection.** This section presents experiments using the VisDrone-DET dataset, where the PP-YOLOE-SOD model is trained and evaluated. The model is trained for 300 epochs using pre-trained weights from the COCO dataset. Experimental results show that the PP-YOLOE-SOD model demonstrates superior performance in small object detection, achieving notable improvements in detection precision and recall across various challenging scenarios and target sizes.

4.2.1. *Implementation details.* This experiment uses the VisDrone-DET dataset for model training and validation. Specifically, the train subset is split for training, while the val subset is used for validation. The experimental environment is configured with the Ubuntu 20.04.5 LTS operating system, a 12th Gen Intel(R) Core(TM) i5-12400 processor, and an NVIDIA GeForce RTX 3090 GPU. The deep learning framework is PaddlePaddle-GPU 2.5.1, accelerated by CUDA 11.1. Relevant parameters are optimized prior to training: the batch size per GPU is set to 8, the model is trained for 300 epochs, and the learning rate is set to 0.00125. The loss function weights α, β and γ are set to 1.0, 2.5, and 0.5, respectively.

4.2.2. *Detection performance analysis.* To evaluate the real-world applicability and performance of PP-YOLOE-SOD, representative and challenging images selected from the VisDrone-DET dataset are used for evaluation. The results, shown in Figure 10, highlight that PP-YOLOE-SOD exhibits exceptional detection capability across UAV images

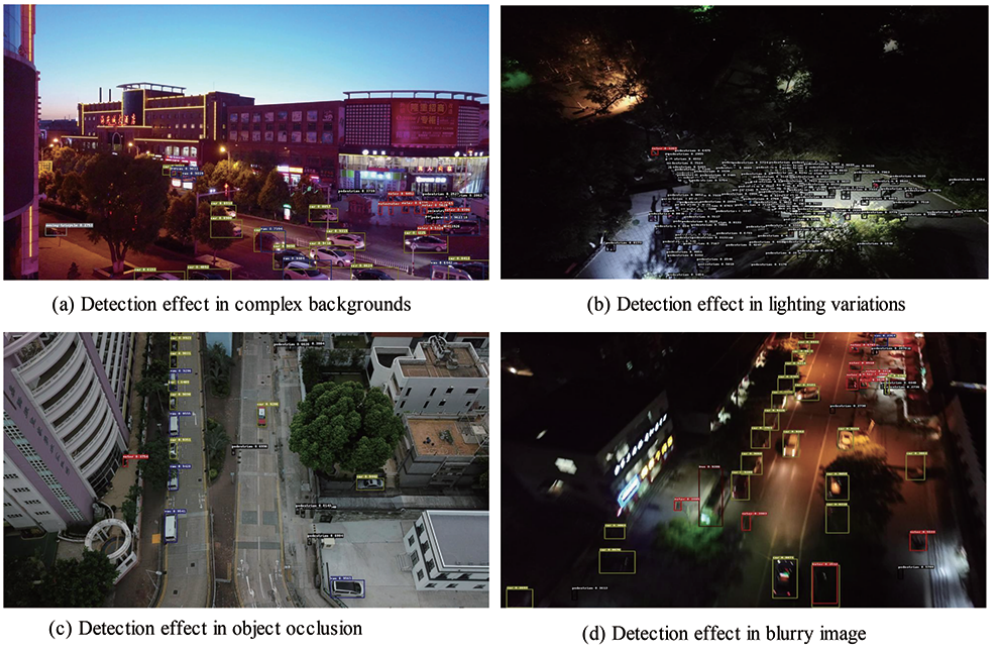

FIGURE 10. Detection effect in different scenarios

with varying shooting angles, lighting conditions, target occlusions, and complex or dense backgrounds. It effectively detects more small and distant targets, suppresses noise interference from buildings, trees, and other background elements, correctly classifies and locates targets, and selectively extracts features crucial for UAV object detection tasks.

Figure 10(a) demonstrates the detection performance of the PP-YOLOE-SOD model in scenes with complex backgrounds. Despite the presence of numerous buildings and lights, the model accurately identifies and localizes vehicles and pedestrians, highlighting its robust detection capability in challenging environments. Figure 10(b) depicts the detection results under varying lighting conditions. The model reliably detects multiple targets even in unevenly illuminated nighttime scenarios. Figure 10(c) illustrates the model's performance in handling target occlusion. It successfully detects and localizes targets even when partially occluded, showcasing its superior capability in managing occlusions. Figure 10(d) evaluates the model's detection performance on blurred images. Despite motion-induced or other forms of blurriness, the model effectively detects multiple targets, maintaining high detection accuracy under poor image clarity.

4.2.3. *Model training results and performance evaluation.* During training, the overall loss steadily decreased, indicating continuous optimization of the model. Similarly, the classification loss showed a progressive decline, demonstrating improved accuracy in target identification and classification. These trends are depicted in Figures 11 and 12, which

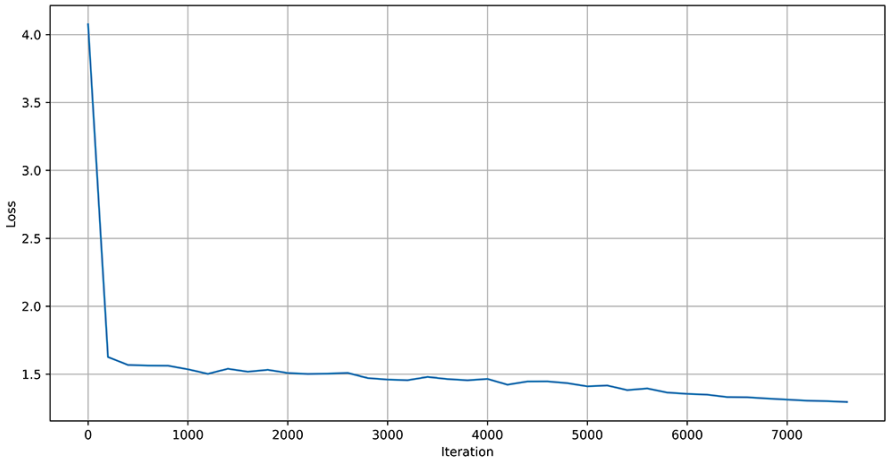

FIGURE 11. Training loss

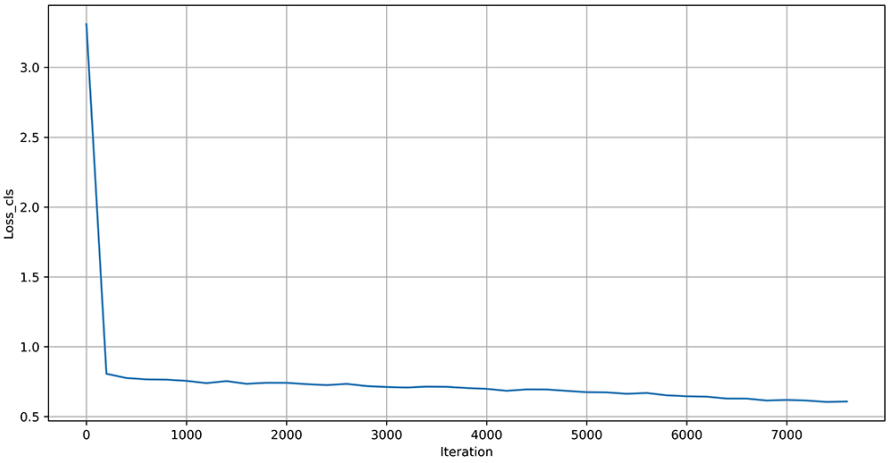

FIGURE 12. Classification loss

clearly illustrate the convergence of the loss functions and the enhancement of classification performance.

In small object detection, challenges such as false positives and missed detections are common, necessitating a thorough evaluation of model accuracy. Average Precision (AP) is a metric used to assess the performance of object detection algorithms for individual categories, measuring precision across different thresholds. Average Recall (AR) indicates the proportion of actual targets successfully detected by the model relative to the total number of targets. To evaluate the model's performance across targets of varying sizes, objects are divided into size-based categories, referred to as target size regions. The PP-YOLOE-SOD model is evaluated on the val subset of the segmented VisDrone-DET dataset, with the results shown in Table 5.

Table 5. Results of the experimental evaluation

	IoU	Area	MaxDets	Results
Average Precision (AP)	0.50:0.95	All	100	0.361
	0.50	All	100	0.572
	0.75	All	100	0.376
	0.50:0.95	Small	100	0.266
	0.50:0.95	Medium	100	0.492
	0.50:0.95	Large	100	0.650
Average Recall (AR)	0.50:0.95	All	1	0.185
	0.50:0.95	All	10	0.459
	0.50:0.95	All	100	0.554
	0.50:0.95	Small	100	0.479
	0.50:0.95	Medium	100	0.679
	0.50:0.95	Large	100	0.807

The results indicate that the model performs well with varying object sizes and Maximum Detection counts (MaxDets). At higher IoU (Intersection over Union) thresholds (0.50:0.95), the model achieves consistently high AP and AR, demonstrating precise target localization and effective detection across different scales. Overall, these findings highlight the model's strong capability in UAV-based ground small object detection tasks.

4.3. **Simulation analysis.** This experiment takes the DJI Matrice 210 RTK UAV as a reference. In the simulation experiment, we set initial conditions similar to those in actual operations and simulated the UAV's operation under these conditions. Specifically, we extracted a particular scenario from the simulation process for a detailed case analysis to better understand the UAV's behavior patterns and response mechanisms under specific conditions. As shown in Figure 13, the simulation results of these scenarios provide important data support and visual evidence for further analysis of UAV performance.

Assume the UAV fails and descends in a ballistic trajectory at this location. Using the standard crash location as the center, simulation results show areas of $S_\sigma = 19.45$ m^2, $S_{2\sigma} = 77.79$ m^2, $S_{3\sigma} = 175.02$ m^2. Risk values are calculated based on target categories and crash probabilities within the impact area. No individuals are present in the one-sigma elliptical region. Between the one-sigma and two-sigma ellipses, four individuals have a risk value of 4.4 each, categorized as severe hazard according to accident severity standards and represented in red. Between the two-sigma and three-sigma ellipses, two individuals have a risk value of 0.8 each, categorized as minor hazard and represented in green. The crash impact area is visualized with severity-based risk representations, as shown in Figure 14.

FIGURE 13. Simulation example of UAV flight process

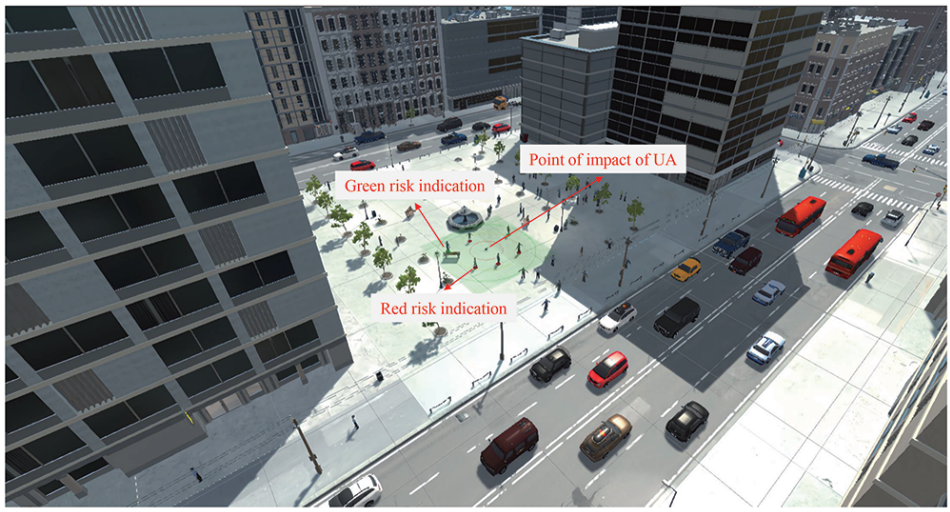

FIGURE 14. Risk representation of UAV crash impact area

These results demonstrate that UAV descent dynamics-based risk modeling combined with target detection effectively assesses crash severity. This approach provides theoretical and standard support for the safe operation of UAVs in complex low-altitude environments, enhancing operational safety and reliability. Future research could optimize the risk assessment model further by incorporating additional environmental variables and dynamic factors to improve its accuracy and applicability.

5. **Conclusion.** In the field of unmanned traffic management, ensuring the safe integration of Unmanned Aerial Systems (UAS) into the national airspace system is essential, with risk assessment playing a vital role in this process. This study combines the dynamic characteristics of UAV descent with object detection technology to propose a comprehensive method for assessing ground risk posed by UAVs. The proposed method addresses uncertainties in UAV crashes and employs object detection technology to identify objects in the crash area, enabling more accurate risk assessment. Through the integration of probabilistic risk assessment, Monte Carlo simulation, and deep learning, a dynamic and adaptive risk assessment model is developed, capable of updating and optimizing based on UAV system failure modes and flight environment data.

1) A risk modeling approach combining UAV descent dynamics and object detection is proposed. This approach accounts for uncertainties during the UAV descent process while considering ground object information within the crash area. By integrating accident severity standards with the model results, the risk value during UAV operations can be determined, which is critical for ensuring operational safety.

2) Using a specific UAV operational scenario as an example, and referencing the DJI Matrice M210-RTK UAV, the feasibility of the proposed risk assessment method is validated.

Although this study provides a preliminary foundation for both theory and practice in UAV ground risk assessment, several important directions remain for further exploration and in-depth research. First, future work could focus on developing a multi-factor collaborative risk assessment model, which would take account of the flight environment, UAV design, and other relevant operational risk factors, thereby enhancing both the comprehensiveness and accuracy of risk evaluations. Second, future research could expand to include real-time adaptive updating mechanisms. By integrating advanced machine learning techniques, such mechanisms would enable dynamic optimization of risk assessments through the real-time acquisition of flight data and environmental information, addressing emerging flight risks as they occur.

As UAV group applications become more widespread, the current methods for assessing the risks of individual UAVs may be less effective in large-scale group operations. Therefore, future research could explore a collaborative risk assessment model based on group behavior, focusing on the interactions between UAVs and their collective impact on ground risks. Such a model would offer more robust theoretical support for the safe operation of large-scale UAV systems. Finally, as UAV technology advances and applications diversify, the development of regulations and standardization within the industry becomes increasingly critical. In this context, integrating the risk assessment model proposed in this study could help promote standardization efforts in the UAV sector, particularly in national airspace management and regulatory frameworks, providing valuable theoretical guidance for the safe integration and sustainable development of UAV technologies.

Acknowledgment. This study received partial funding from the National Natural Science Foundation of China (Grant No. U2133208). The authors sincerely appreciate the generous financial support provided by the National Natural Science Foundation, which played a crucial role in the successful completion of this research.

REFERENCES

[1] E. P. Cabrera, J. S. Agila, F. Astudillo-Salinas, A. Vazquez-Rodas, S. P. Torres and I. Minchala-Avila, Data collection using unmanned aerial vehicles and a delay-tolerant network, *International Journal of Innovative Computing, Information and Control*, vol.19, no.5, pp.1337-1360, DOI: 10.24507/ijicic.19.05.1337, 2023.

[2] D. A. Tyas, I. Candradewi, B. Baskara, N. P. Indarto, H. Abdurrahman, Y. Argha, B. A. A. Sumbodo and A. Dharmawan, Horizon detection for UAV attitude based on image processing approach, *ICIC Express Letters*, vol.16, no.12, pp.1249-1258, DOI: 10.24507/icicel.16.12.1249, 2022.

[3] Q. Zhou, J. W. Zhang and G. C. Liu, Risk analysis of unmanned aerial system operation, *Proceedings of the World Transportation Engineering and Technology Forum (WTC2021)*, Beijing, China, pp.2480-2484, 2021.

[4] X. Li, X. Sun and M. Fang, Risk assessment of unmanned aerial vehicle (UAV) operations based on Bayesian network, *2022 2nd International Conference on Big Data, Artificial Intelligence and Risk Management (ICBAR)*, Xi'an, China, pp.189-193, DOI: 10.1109/ICBAR58199.2022.00043, 2022.

[5] H. Li and F. Y. Nie, Collision risk assessment of logistics UAV based on Bayesian network, *Science Technology and Engineering*, vol.23, no.15, pp.6700-6706, 2023.

[6] P. Han, X. Yang, Y. Zhao, X. Guan and S. Wang, Quantitative ground risk assessment for urban logistical unmanned aerial vehicle (UAV) based on Bayesian network, *Sustainability*, vol.14, 5733, DOI: 10.3390/su14095733, 2022.

[7] Y. Liu, X. Zhang, Z. Wang, Z. Gao and C. Liu, Ground risk assessment of UAV operations based on horizontal distance estimation under uncertain conditions, *Mathematical Problems in Engineering*, 3384870, DOI: 10.1155/2021/3384870, 2021.

[8] Joint Authorities for Rulemaking of Unmanned Systems, *JARUS Guidelines on Specific Operations Risk Assessment (SORA)*, D.04, Cologne, 2019.

[9] Civil Aviation Administration of China, *Trial Operation Management Regulations for Specific Types of Unmanned Aircraft (Interim)*, AC-92-2019-01, Beijing, 2019.

[10] Civil Aviation Administration of China, Aircraft Airworthiness Certification Department, *Guidance on Unmanned Aircraft Airworthiness Certification Based on Operational Risk*, Beijing, 2019.

[11] Z. Oudina, M. Derdour, A. Dib and M. M. Bouhamed, Empirical analysis of the security threats and risks that drones face, represent, and mitigation, *2024 6th International Conference on Pattern Analysis and Intelligent Systems (PAIS)*, EL OUED, Algeria, pp.1-8, DOI: 10.1109/PAIS62114.2024.10541193, 2024.

[12] G. Gigante, M. Bernard, R. Palumbo, L. Travascio and A. Vozella, Current approaches in UAV operational risk assessment and practical considerations, *Journal of Physics: Conference Series*, https://api.semanticscholar.org/CorpusID:268475648, 2024.

[13] A. La Cour-Harbo, Ground impact probability distribution for small unmanned aircraft in ballistic descent, *2020 International Conference on Unmanned Aircraft Systems (ICUAS)*, Athens, Greece, pp.1442-1451, DOI: 10.1109/ICUAS48674.2020.9213990, 2020.

[14] W. T. Wang, X. S. Gan, Y. R. Wu, J. S. Ren and C. X. Wang, Low-altitude UAV operation risk assessment method considering the uncertainty, *Modern Defense Technology*, vol.50, no.5, pp.14-21, 2022.

[15] L. Tong, X. Gan, Y. Wu and H. Zhang, Identification of safety factors for UAV systems in non-isolated airspace, *2022 International Conference on Information System, Computing and Educational Technology (ICISCET)*, Montreal, QC, Canada, pp.232-236, DOI: 10.1109/ICISCET56785.2022.00063, 2022.

[16] T. Serru and K. Delmas, A comprehensive probabilistic assessment method of UAS ground collision risk, *The 31st European Safety and Reliability Conference (ESREL)*, Angers, France, pp.38-45, 2021.

[17] J. Bu, H. H. Zhang, M. H. Hu et al., Risk assessment of unmanned aerial vehicle flight based on K-means clustering algorithm, *Transactions of Nanjing University of Aeronautics and Astronautics*, vol.37, no.2, pp.263-273, 2020.

[18] R. H. Jaime, G. Abhishek and O. Yew, Data-driven risk assessment and multicriteria optimization of UAV operations, *Aerospace Science and Technology*, vol.77, pp.510-523, DOI: 10.1016/j.ast.2018.04.001, 2018.

[19] Q. Jiao, Y. Liu, Z. Zheng, L. Sun, Y. Bai, Z. Zhang, L. Sun, G. Ren, G. Zhou, X. Chen et al., Ground risk assessment for unmanned aircraft systems based on dynamic model, *Drones*, vol.6, 324, DOI: 10.3390/drones6110324, 2022.

[20] Y.-C. Lai and T.-Y. Lin, Vision-based mid-air object detection and avoidance approach for small unmanned aerial vehicles with deep learning and risk assessment, *Remote Sens.*, vol.16, 756, DOI: 10.3390/rs16050756, 2024.

[21] A. K. Sivakumar, M. H. C. Man and K. H. Low, Preliminary ground risk tiering for small unmanned aerial vehicles (sUAV) in metropolitan environments, *2022 International Conference on Unmanned Aircraft Systems (ICUAS)*, Dubrovnik, Croatia, pp.1083-1090, DOI: 10.1109/ICUAS54217.2022.9836157, 2022.

[22] G. Zhong, J. Li, X. W. Zhang et al., A risk assessment method of logistics drones on ground, *Journal of Transportation Systems Engineering and Information Technology*, vol.22, no.4, pp.246-254, 2022.

[23] S. Primatesta, G. Guglieri and A. Rizzo, A risk-aware path planning strategy for UAVs in urban environments, *Journal of Intelligent & Robotic Systems*, vol.95, pp.629-643, DOI: 10.1007/s10846-018-0924-3, 2019.

[24] S. Primatesta, A. Rizzo and A. La Cour-Harbo, Ground risk map for unmanned aircraft in urban environments, *Journal of Intelligent & Robotic Systems*, vol.97, pp.489-509, DOI: 10.1007/s10846-019-01015-z, 2020.

[25] G. Avanzini and D. S. Martínez, Risk assessment in mission planning of uninhabited aerial vehicles, *Proceedings of the Institution of Mechanical Engineers, Part G: Journal of Aerospace Engineering*, vol.233, no.10, pp.3499-3518, 2019.

[26] F. Q. Qi, Study on ground impact risk of UAS based on operational scenarios, *Industrial Safety and Environmental Protection*, vol.48, no.10, pp.17-20+31, 2022.
[27] P. Han and Y. F. Zhao, Study on ground impact risk of UAV based on flight environment, *China Safety Science Journal*, vol.30, no.1, pp.142-147, 2020.
[28] Z. J. Zhang, S. G. Zhang, X. Liu and L. Jin, Estimated method of target level of safety for unmanned aircraft system, *Journal of Aerospace Power*, vol.33, no.4, pp.1017-1024, DOI: 10.13224/j.cnki.jasp.2018.04.029, 2018.
[29] A. McFadyen, T. Martin and T. Perez, Low-level collision risk modelling for unmanned aircraft integration and management, *2018 IEEE Aerospace Conference*, pp.1-10, 2018.
[30] S. Zhou, Y. Liu, X. Zhang, H. Dong, W. Zhang, H. Wu and H. Li, Risk assessment and distribution estimation for UAV operations with accurate ground feature extraction based on a multi-layer method in urban areas, *Drones*, vol.8, 399, DOI: 10.3390/drones8080399, 2024.
[31] A. La Cour-Harbo, Quantifying risk of ground impact fatalities for small unmanned aircraft, *Journal of Intelligent & Robotic Systems*, vol.93, pp.367-384, DOI: 10.1007/s10846-018-0853-1, 2019.
[32] Y. J. Zhu, Y. Li, Z. A. Gao, Y. Liu and X. J. Zhang, A review of UAS route planning in urban airspace with acceptable risk levels, *Journal of Xihua University (Natural Science Edition)*, vol.41, no.1, pp.7-12, 2022.
[33] P. Han and B. Y. Zhang, Effect of track error on safety risk assessment of UAV ground impact, *China Safety Science Journal*, vol.31, no.2, pp.106-111, 2021.
[34] C. Ma, Y. Fu, D. Wang, R. Guo, X. Zhao and J. Fang, YOLO-UAV: Object detection method of unmanned aerial vehicle imagery based on efficient multi-scale feature fusion, *IEEE Access*, vol.11, pp.126857-126878, DOI: 10.1109/ACCESS.2023.3329713, 2023.
[35] P. F. Zhu, L. Y. Wen, D. W. Du, X. Bian, H. Fan, Q. H. Hu and H. B. Ling, Detection and tracking meet drones challenge, *IEEE Transactions on Pattern Analysis and Machine Intelligence*, vol.44, no.11, pp.7380-7399, DOI: 10.1109/TPAMI.2021.3119563, 2022.
[36] F. C. Akyon, S. O. Altinuc and A. Temizel, Slicing aided hyper inference and fine-tuning for small object detection, *2022 IEEE International Conference on Image Processing (ICIP)*, pp.966-970, DOI: 10.1109/ICIP46576.2022.9897990, 2022.
[37] G. S. Xia, X. Bai, J. Ding et al., DOTA: A large-scale dataset for object detection in aerial images, *Proc. of the IEEE Conference on Computer Vision and Pattern Recognition*, pp.3974-3983, 2018.
[38] S. L. Xu, X. X. Wang, W. Y. Lv et al., PP-YOLOE: An evolved version of YOLO, *arXiv Preprint*, arXiv: 2203.16250, 2022.
[39] Q. Quan, G. Li, Y. Q. Bai, R. Fu, M. X. Li, C. X. Ke et al., Low altitude UAV traffic management: An introductory overview and proposal, *Acta Aeronauticaet Astronautica Sinica*, vol.41, no.1, DOI: 10.7527/S1000-6893.2019.23238, 2020.

Author Biography

Sen Luo obtained his Bachelor's degree in Computer Science and Technology from Sichuan Minzu College in 2022. He is currently pursuing a Master's degree at the School of Computer Science, Chengdu University of Information Technology, with an expected graduation date of 2025. His research interests include UAV operational risk assessment and deep learning.

Xingyu Cao obtained his Bachelor's degree in Software Engineering from Chengdu University of Information Technology in 2022. He is currently a Master's student at the School of Computer Science, Chengdu University of Information Technology, expected to graduate in 2025. His research interests include pedestrian re-identification and UAV operational risk assessment.

Qinggang Wu obtained his Bachelor's degree from Nanjing University of Aeronautics and Astronautics in 2016 and his Master's degree from the same university in 2019. He is currently an assistant researcher at the Second Research Institute of the Civil Aviation Administration of China. His current research interests include remote and unmanned air traffic control technology.

Pengxin Ding studied at the School of Computer Science (Software) at Sichuan University from 2016 to 2020, where he earned his Ph.D. degree. He is currently an associate researcher at the School of Computer Science, Chengdu University of Information Technology. He has been engaged in long-term research on artificial intelligence and informatization, with a focus on applying research outcomes in fields such as transportation and healthcare. His research interests include UAV operational management, artificial intelligence, and informatization.